Journal of Materials Chemistry C

Accepted Manuscript

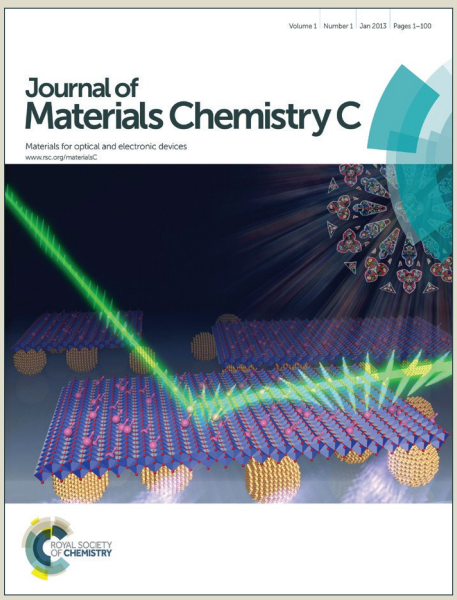

ROYAL SOCIETY OF CHEMISTRY

www.rsc.org/materialsC

Journal Name

RSCPublishing

ARTICLE

Moisture-induced degradation and its mechanism of $(Sr,Ca)AlSiN_3:Eu^{2+}$, a red-color-converter for solid state lighting

Cite this: DOI: 10.1039/x0xx00000x

Received 00th January 2012,
Accepted 00th January 2012

DOI: 10.1039/x0xx00000x

www.rsc.org/

Jie Zhu[a,b], Rong-Jun Xie[a, c]*, Tianliang Zhou[c], Yujin Cho[d,e], Takayuki Suehiro[a], Takashi Takeda[a], Ming Lu[b], Takashi Sekiguchi[d,e], Naoto Hirosaki[a]

$(Sr,Ca)AlSiN_3:Eu^{2+}$ (SCASN) is a very promising red phosphor used as a down-conversion luminescent material in solid state lighting. In this study, the moisture-induced degradation of SCASN was comprehensively investigated by treating it under a severe condition of high-pressure water steam. The degradation initiated at 150°C, and the luminescence of SCASN was seen to be quenched quickly, with the powder sample being bleached after the treatment. Both of the microstructure and phase changed obviously with the oxidation, and the host turned finally into NH_3, $(Sr,Ca)Al_2Si_2O_8$ and $Ca(OH)_2$. By using a variety of spectroscopic, surface and microstructure analytic techniques, the degradation mechanism was clarified and proposed to occur *via* the oxidant-gas penetration mechanism through the moisture-enhanced oxidation of both the SCASN host and divalent europium. The activation energy for the moisture-induced degradation was about 66.32 kJ.

Introduction

With materials becoming an indispensable ingredient in human life, material chemistry has been extensively studied covering many aspects including synthesis, property, application, stability and so on. Controlling the stability is a primary requisite for material applications. On the other hand, as an irreversible transformation, the degradation has gained great concern, because it significantly hinders the stability of materials, and thus makes them become defunctionalized. Degradation may occur in different ways depending upon the nature of the causing agents, such as thermal, photo-, oxidation- and moisture-induced degradations and so on.[1,2] A better understanding of degradation mechanisms should be advocated in order to facilitate the proper use of a material.

Phosphors are high-purity luminescent materials that emit light when exposed to excitation sources such as photons, electrons or an electric field. Among a large number of phosphors that have been discovered or developed, (oxy)nitride ones are considered as very promising down-conversion luminescent materials in solid state lighting, owing to their high quantum efficiency, high chemical stability as well as small thermal quenching or degradation.[3-5] Notable examples include $MSi_2O_2N_2$: Eu^{2+} (M=Ca, Sr, Ba),[6,7] $M_2Si_5N_8$: Eu^{2+} (M= Ca, Sr, Ba),[8-10] α-SiAlON: Eu^{2+}, [11,12] β-sialon:Eu^{2+},[13] $CaAlSiN_3:Eu^{2+}$,[14] and so on. In recent years, $CaAlSiN_3$ has drawn much attention for its application in warm white or high color rendition LEDs because it is a highly efficient orange or red phosphor with high quenching temperature.[14-17] Various researches have been devoted to the synthesis, structure, luminescence properties, and applications of $CaAlSiN_3$. [14-19] On the other hand, besides the parameters of luminescence spectra, quantum efficiency and thermal quenching, luminescence degradation is a big challenge, preventing phosphor from commercialization.[20] Degradation as an irreversible transformation is different from luminescence quenching, so that only thermal quenching is not sufficient for evaluating a phosphor, and thermal- or moisture-induced degradation should also be investigated.[21]

Usually, the reliability of phosphors for use in solid state lighting is evaluated by the sequential damp heat (85°C/85%) tests which last at least 1,000 h. In order to have a sense of the reliability of a phosphor shortly, the testing time should be significantly reduced. In other words, much higher temperature and humidity are required in the test experiments for saving time. Although it is not an industrial standard, it makes sense to understand the luminescence degradation and phase evolutions of nitride phosphors under the high-pressure water steam condition. In the present work, the degradation behavior of the Sr-substituted $CaAlSiN_3:Eu^{2+}$ will be evaluated by treating the phosphor under a severe condition of high humidity, vapor pressure and temperature. With the partial replacement of Ca by Sr, the luminescence is blue shifted.[17] The photoluminescence, cathodoluminescence, and microstructure of the treated samples will be analyzed, and the degradation mechanism will be elucidated and discussed. It is believed that the phosphor can be

treated in a better way if mechanistic implications of degradation are properly understood. The concept also works for other phosphors and this study may play a directive role in phosphor development in the future.

Experimental Section

Material and characterization

The Sr-substituted $CaAlSiN_3$ phosphor with the composition of $(Sr_{0.4}Ca_{0.592})AlSiN_3:Eu_{0.008}$ (SCASN) was prepared by firing the powder mixture of Sr_3N_2, Ca_3N_2, EuN, AlN, Si_3N_4 at 1800°C for 2 h under the 1.0 MPa N_2 atmosphere. The photoluminescence (PL) spectra were measured at room temperature by a fluorescent spectrophotometer (FL-4500, Hitachi Ltd., Japan) with a 200 W Xe-lamp as an excitation source. XRD patterns were collected with Rigaku, RINT Ultima-III using Cu K_a radiation at 40 kV and 40 mA. The concentration of elements (*i.e.*, Sr, Ca, Al, Si, Eu) was estimated by inductively coupled plasma atomic emission spectroscopy (ICP), and the O and N contents were measured by the N/O analyzer (TC-436, LECO Co.). X-ray photoelectron spectroscopy (XPS) was recorded through PHI Quantera SXM (ULVAC-PHI) using Al K_a mono X-ray radiation at 20 kV and 5 mA. SEM images were taken on JEOLJSM-6380LV. Cathodoluminescence (CL) was detected by Horiba MP32S/M at 5 kV. Energy dispersive spectrometer (EDS) analyses were carried out with Hitachi S4800.

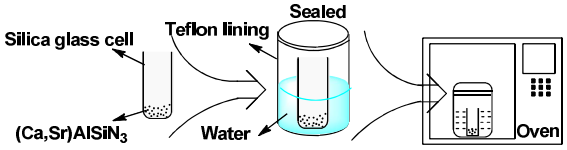

Fig. 1 Schematics of the moisture-induced degradation process.

General procedure for the degradation reaction

Reactions were carried out in an autoclave with Teflon lining. Moisture-induced degradation process was shown in Fig. 1. About 1 g SCASN was put into a glass bottle (silica glass cell) which placed in an autoclave. 20 mL water was added to the autoclave, so that the bottle was immersed in water while the phosphor did not contact with water directly. Afterwards, the sealed autoclave was loaded in an oven at a constant temperature for a certain time period. After the experiment, the samples were cooled down to room temperature with the furnace, and dried at 100°C overnight in a N_2 flowing muffle furnace for spectroscopy and microstructure investigations.

Results and Discussion

Luminescence degradation

In the moisture-induced degradation experiment, both of the humidity and pressure in the autoclave containing the phosphor powder would increase as the temperature increases. For comparison, thermal-induced degradation was conducted by baking the phosphor powder in air.

Figure 2 shows the photoluminescence (PL) spectra of SCASN baked for 8 h at varying temperatures. It can be seen that the phosphor starts to degrade in photoluminescence slightly at around 200°C, indicating a good thermal stability of SCASN when heated in dry air. On the other hand, the luminescence intensity of samples treated in moisture declines initially at about 150°C, and drops quickly thereafter. The luminescence losses by 30% at 200°C for samples treated in moisture (*vs* 2% in dry air). The great difference in both initial degradation temperature and the degree of luminescence loss indicates that the samples are more easily attacked by the high-pressure steam.

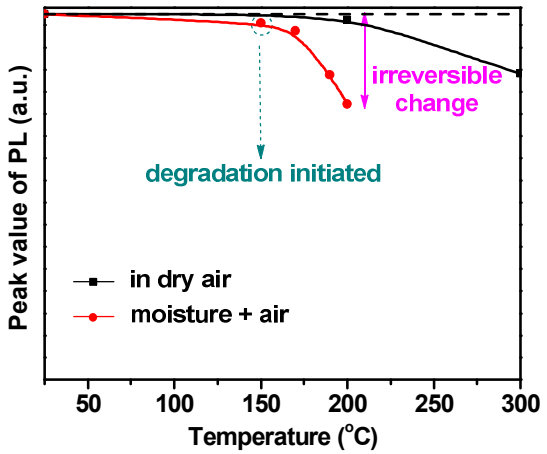

Fig. 2 Degradation of $(Sr,Ca)AlSiN_3$ baked in dry air and treated in water steam at different temperatures for 8h, indicating thermal- and moisture-induced luminescence loss, respectively.

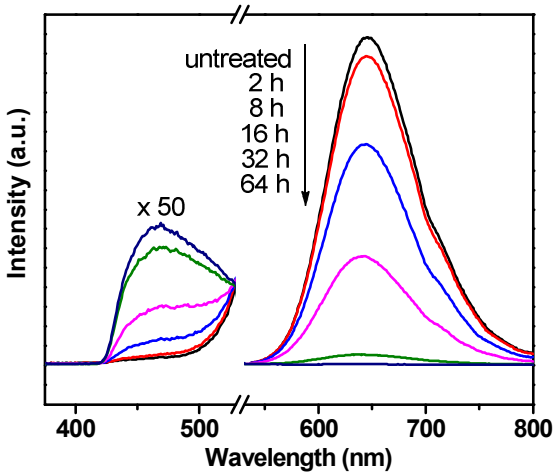

Fig. 3 Emission spectra of SCASN treated in moisture at 200°C for different time periods. Samples were excited at λ_{em} = 365 nm.

The influence of reaction time on degradation was also studied (Fig. 3). As expected, the degradation becomes more serious with increasing the dwell time at a certain temperature. It can also be reflected from the sample colour that bleaches out gradually. The luminescence property almost disappears after treated for 64 h at 200°C, with the sample colour turning into white. On the other hand, it is worth noting that when the phosphor is excited by 365 nm, another emission peak appears at 400~500 nm (Fig. 3), the intensity of which tends to increase along with the reaction time. It is attributed to a second phase that produces gradually during the degradation process. The second phase shows a different emission spectrum from the original SCASN, which has a negative influence on the luminescence of the phosphor investigated, such as chromatic coordination, thermal stability, reliability and *etc*.

Chemical composition analysis

To obtain more information of the second phase, the elemental analyses were applied to the samples treated for 16 h at 170, 190, 200°C, respectively. The normalized results are listed in Table 1. It is seen that the molar ratio of (Ca+Sr): Si: Al remains almost constant for samples treated at different temperatures, whereas the contents of N and O vary obviously. With the degradation proceeding, the N percentage decreases greatly while that of O enhances remarkably, indicating that the moisture-induced oxidation occurs. Considering the fact that the solution in autoclave presents alkalinity after reaction, ammonia (NH_3) is supposed to be produced, carrying N away from the host. Simultaneously, a new silicate phase is generated, gaining O probably from the moisture (H_2O).

Table 1 Elemental analyses of SCASN treated in moisture for 16 h (wt%).

	Ca	Sr	Eu	Si	Al	N	O
untreated	12.8	22.9	0.70	18.3	18.0	26.3	1.0
170°C	11.4	20.5	0.67	16.5	16.1	15.6	19.3
190°C	10.6	19.2	0.58	15.5	15.0	7.0	32.4
200°C	10.1	18.3	0.56	14.6	14.1	4.5	37.6

To further confirm the second phase generated, XRD analyses were performed for the samples after treating at 200°C, as shown in Fig. 4. It is seen that, the untreated sample is of good crystallinity, consisting of the main phase SCASN and a trace amount of residual AlN phase (labelled by the arrow). There is no obvious phase evolution detected even for sampled treated in moisture for 16 h, with only reduction in peak intensity. It is in a good agreement with the reduction in photoluminescence intensity (Fig. 3). After that, a transition state of an amorphous phase seems to appear at 32 h and only a broad feature is seen at about 2θ = 28°. It is conjectured that the generated second phase with a very small particle size is not of crystalline form, and deposits on the surface of SCASN. For samples treated for a longer time, diffraction peaks sharpens again, signifying that SCASN is totally destroyed and the generated second phase finally grows into crystal grains. XRD patterns of the sample after treating for 64 h and 100 h coincide well with the standard data for $SrAl_2Si_2O_8$ (PDF No. 35-0073). [22] The emission of $SrAl_2Si_2O_8$: Eu^{2+} was reported to be around 440 nm, which matches with the blue emission seen in Fig.3.[23] Although it is not identified from the XRD patterns, $Ca(OH)_2$ is also supposed to be generated during the moisture-induced oxidation (discussion later).

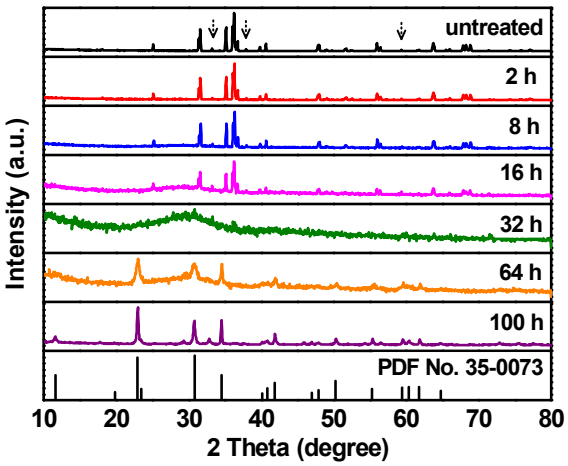

Fig. 4 XRD patterns of SCASN treated in moisture at 200°C.

Activation energy for the moisture-induced degradation

To explore the reaction mechanism, the calculation of the activation energy E_a for the degradation was attempted, according to Arrhenius Equation:

$$k = Ae^{-E_a/RT} \quad (1)$$

Where k is the reaction rate, determined through the reduction of PL intensity here, A is the Arrhenius constant, R the universal gas constant, and T the absolute temperature. With the peak value of PL intensity plotted as ordinate and time as abscissa, the data were fitted as shown in Fig. 5(a), and k can be calculated from the slope of line. Good linearity is exhibited in the temperature range of 150-200°C. Arrhenius Equation can be then fitted with ln$k$ as ordinate and 1/T as abscissa, as shown in Fig. 5(b). The activation energy is finally determined to be 66.32 kJ. It means that the degradation process could happen if enough energy is provided. Also, with rising the temperature or prolonging the time, the reaction mechanism does not vary, although the moisture-induced oxidation penetrates from the surface into the inner part of particles.

XPS analysis

The surface states of the phosphor were also investigated by X-ray photoelectron spectroscopy (XPS) analyses. Figure 6 presents the high resolution XPS spectra of N 1s, O 1s, Ca 2p, Sr 3d, and Eu 3d. These spectra were further deconvoluted,

with experimental spectra depicted in dots and simulated one in solid lines, respectively. For the untreated sample, three main peaks deconvoluted from N 1s at 400.25, 396.62 and 397.56 eV are attributed to Sr-N, Si-N and Al-N bond respectively.[23,24] After the moisture treatment, however, N 1s spectra almost disappears. It is attributable to the loss of N by releasing out NH_3, which can be supported by the ICP data.

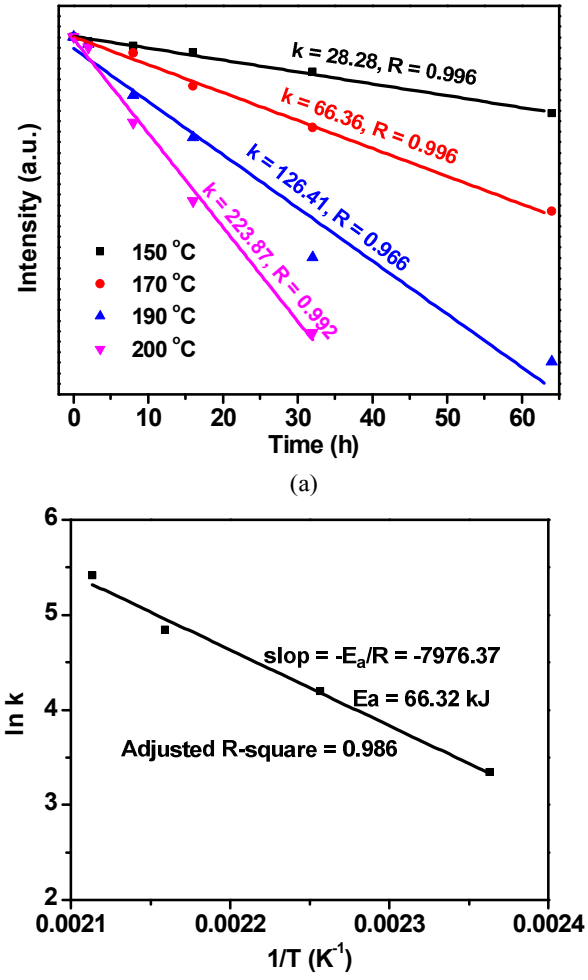

Fig. 5 Calculations of the reaction rate k (a) and the activation energy according to the Arrhenius Equation.

The core level spectra of O 1s (Fig. 6b) can be decomposed into three peaks and the binding energy at 532.16~532.27, 531.32~531.64, 530.30~530.86 eV is assigned to Si-O, Al-O and Sr-O bonds, respectively.[25-27] Different from N 1s spectra, XPS spectra of O 1s become stronger after treatment. As for the Sr 3d XPS spectra (Fig. 6c), the binding energy at 135.12~136.13 and 133.31~134.38 eV is identified to Sr $3d_{3/2}$ and $3d_{5/2}$ respectively. It was reported that the XPS peak positions of Sr 3d shifted to the higher-energy side when it was oxidized.[25,26,28] It is due to the greater electronegativity of oxygen. So in our case, Sr $3d_{3/2}$ can be further deconvoluted into Sr-O ($3d_{3/2}$) and Sr-N ($3d_{3/2}$) at ~136.12 and ~135.13 eV, respectively; and Sr $3d_{5/2}$ into Sr-O ($3d_{5/2}$) and Sr-N ($3d_{5/2}$) at ~134.32 and ~133.31 eV. As seen, the XPS spectrum of Sr 3d shifts to the higher binding energy side, which corresponds to the increasing content of Sr-O and suggests the formation of silicate. The similar results are seen in the Ca case (Fig. 6d). For the Eu 3d XPS spectra (Fig. 6e), two regions at ~1160 and ~1130 eV are attributed to Eu $3d_{3/2}$ and $3d_{5/2}$, respectively.[26] The peaks at 1135.6 and 1125.6 eV are assigned to trivalent and divalent Eu^{2+} ions, respectively.[29-31] As can be seen, the intensity of Eu^{3+} becomes much stronger after treatment, indicative of the oxidation of Eu^{2+}.

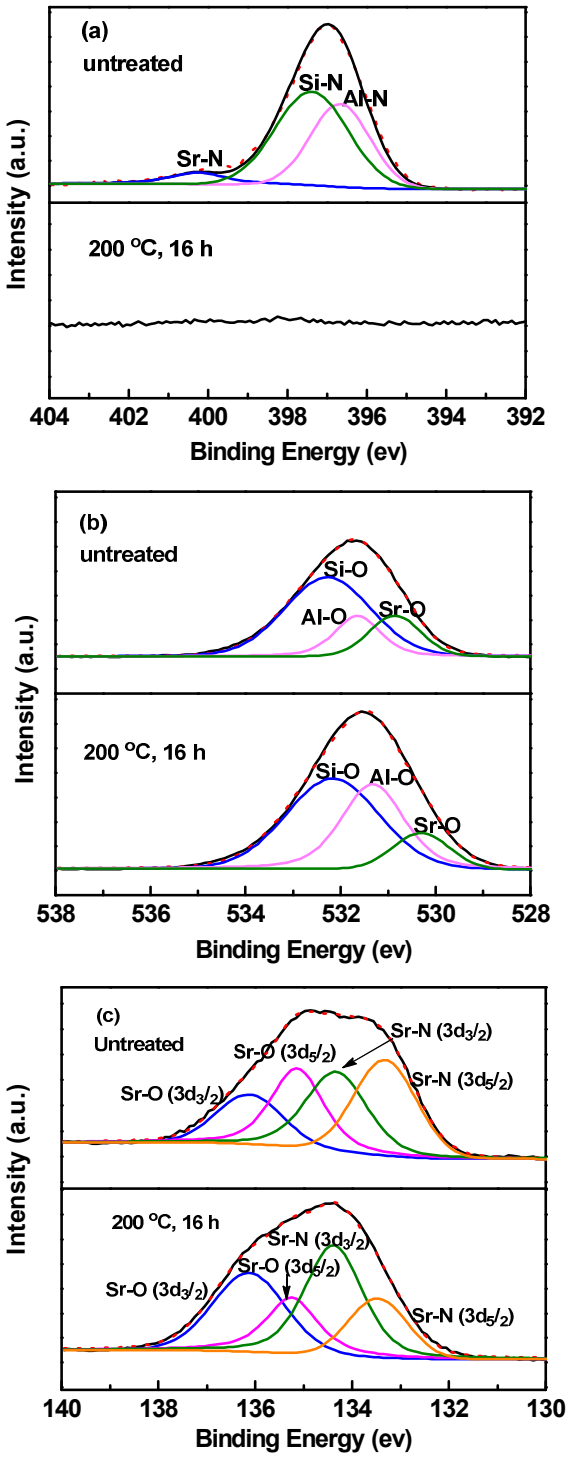

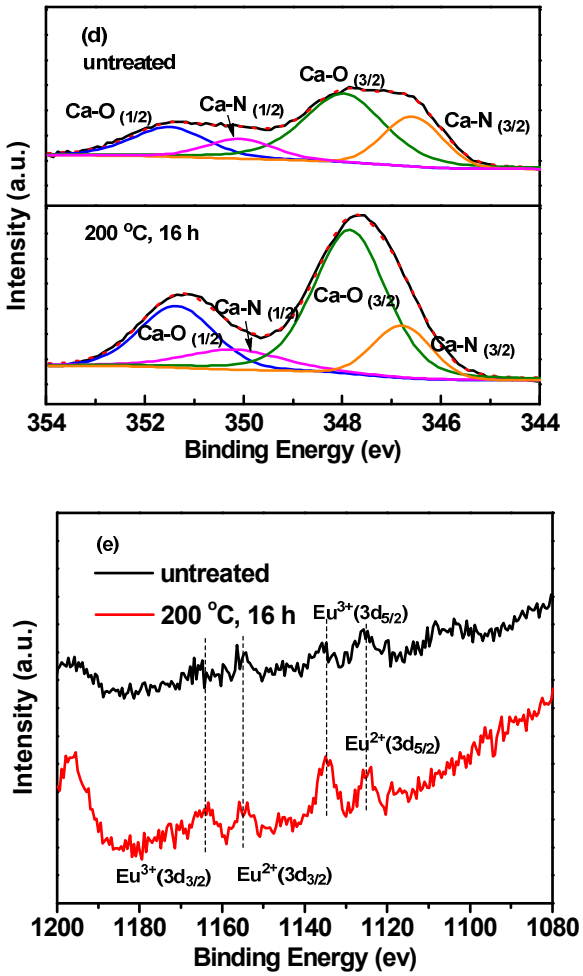

Fig. 6 XPS spectra of N 1s (a), O 1s (b), Sr 3d (c), Ca 2p (d) and Eu 3d (e), respectively.

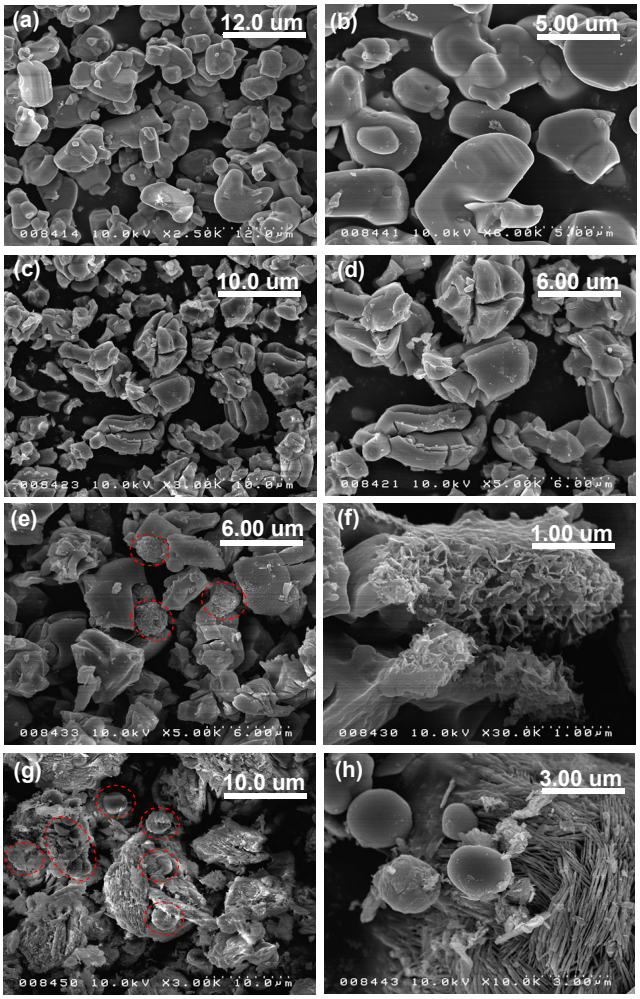

Fig. 7 SEM images of the as prepared SCASN (a) and (b); SCASN after treatment in moisture at 200°C for 16 h (c) and (d), 32 h (e) and (f); 100 h (g) and (h).

SEM observations

As shown in Fig. 7, the as prepared phosphor exhibits a smooth surface and good crystallinity. The particle starts to crack after treatment in moisture for 16 h, but the surface remains smooth after the particle splitting. This corresponds to the reduction in the XRD peak intensity only, and no phase evolutions occur. After 32 h treatment, however, the surface of phosphor fragments is corroded, folded, and cracked. The XRD pattern at this stage shows only a broad peak, due to the formation of amorphous phases. It matches with SEM images since the crystallinity of SCASN is destroyed after treatment for 32 h, and the second phase generated is in the non-crystal form and presents as wrinkles on the surface. While keeping the degradation process moving on, the corrosion penetrates into the inner-face of particles, exhibiting the loose layered morphology as shown in Figs. 7g and 7 h. It can also be seen in XRD patterns at 64 h and 100 h that $SrAl_2Si_2O_8$ forms as a dominant phase. Furthermore, a bubble-like new phase appears, which is thought to be $Ca(OH)_2$ as discussed later.

Cathodoluminescence (CL) and CL mapping

To have an intuitive view of the localized luminescence, CL of treated samples was investigated, as illustrated in Fig. 8. The as-prepared phosphor shows a broad CL spectrum centered at 640 nm, which is due to the emission of Eu^{2+} in SCASN. A very weak CL emission around 350 nm is also observed, originating from the band gap emission of the residual AlN. For the treated samples, several sharp peaks are seen at 600, 610, 650 and 700 nm, which are assigned to the Eu^{3+} luminescence. It clearly indicates that Eu^{2+} is oxidized into Eu^{3+} when samples are treated in moisture. For those samples treated for 16 and 32 h, the CL emission peak around 460 nm is assigned to $SrAl_2Si_2O_8$:Eu^{2+}. After 100 h treatment, however, the blue emission disappears as Eu^{2+} is totally oxidized into Eu^{3+}. Figure 8b shows that the bubble-like particles have no luminescence at all, whereas the broad band at 350 nm and several sharp lines are attributed to the band gap emission of $SrAl_2Si_2O_8$ and the Eu^{3+} emission, respectively.

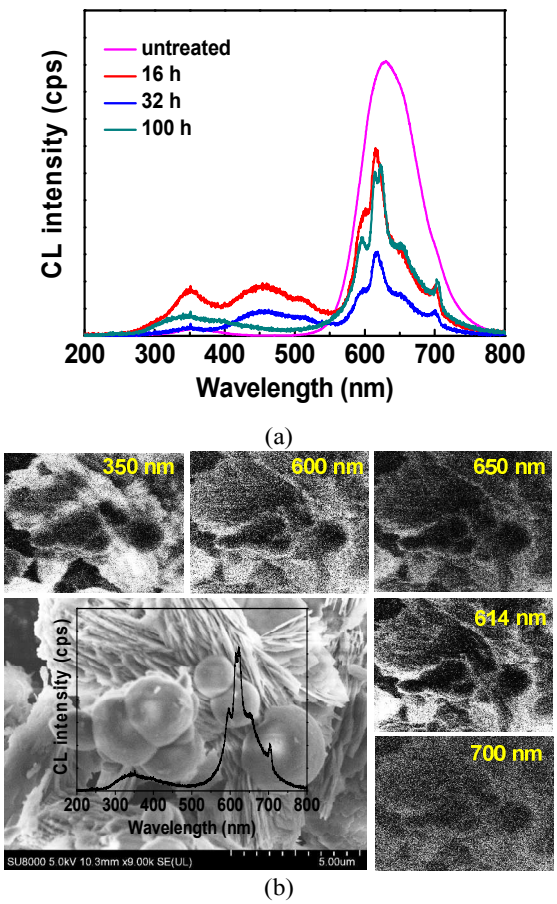

Fig. 8 (a) Cathodoluminescence of SCASN treated in moisture at 200°C for varying dwell times; and (b) cathodoluminescence mapping of the sample treated for 100 h. An acceleration voltage of 5 KV was used.

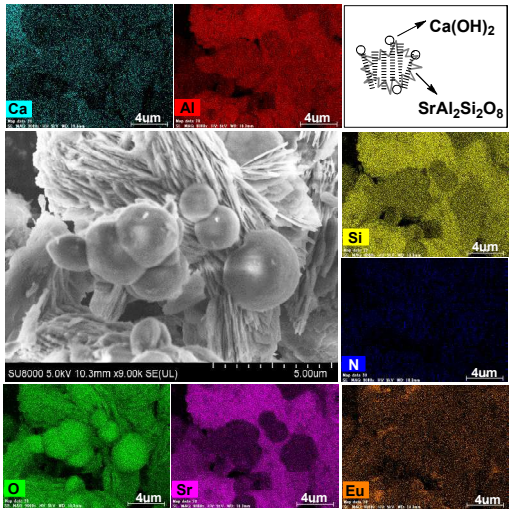

Fig. 9 EDS mapping of SCASN treated at 200°C for 100 h in moisture.

As shown in Fig. 9, the bubble-like spherical particles are enriched in Ca and O, but deficient in Al, Sr, Si and N, which can be supposed to be $Ca(OH)_2$. The matrix with the layered morphology, enriched in Sr, Ca, Al, Si and O, is thus $SrAl_2Si_2O_8$. Therefore, the whole degradation process can be explained as the destruction of the original crystal phase and then the generation of two new crystalline phases of $(Sr,Ca)Al_2Si_2O_8$ and $Ca(OH)_2$.

Moisture-induced degradation mechanism

Investigations on luminescence degradation of phosphors are of an important topic, which would understand the factors controlling the luminescence loss and provide suggestions on materials design and applications. As seen in Fig. 2, treating the red-emitting SCASN phosphor in water steam reduces the initial temperature for luminescence degradation from 200 to 150°C, and accelerates the degradation remarkably. It indicates that the mechanism for the moisture-induced degradation differs from that of the thermal-induced one.

Ikeda and Nii investigated the oxidation reactions of Fe-Cr alloys in dry O_2 and O_2-10% H_2O at high temperature.[32,33] The weight gain in wet oxygen was found to be one order of magnitude greater than that in dry oxygen. A oxidant-gas penetration mechanism was proposed to explain the oxidation behavior of alloys in oxygen containing moisture. Honda *et al.* further confirmed that the supply of oxygen *via* moisture was faster than in dry atmospheres.[34] This mechanism is also true for the moisture-induced degradation of SCASN that is caused by the oxidation of both the host and the activator. It is evidenced by the particle cracking, fragment and the loose layered structure of the silicate. Oxidation initiates at the phosphor particle surface, and then takes place at the inner part of the particle by the oxidant gas penetrating through cracks with the help of moisture (high-pressure water steam). The existence of H_2O leads to the consumption of N in SCASN by releasing NH_3, which again promotes the oxidation process. The results analyzed by the composition, microstructure and cathodoluminescence measurements are indicative of the formation of $(Sr,Ca)Al_2Si_2O_8$, $Ca(OH)_2$ and NH_3 products, so that the following reaction equation for the host oxidation can be put forwarded. Figure 10 presents a schematic view of such a process.

$$2(Ca,Sr)AlSiN_3(s) + 10H_2O(g) \rightarrow (Sr,Ca)Al_2Si_2O_8(s) + 6NH_3\,(g) + Ca(OH)_2\,(s) \quad (2)$$

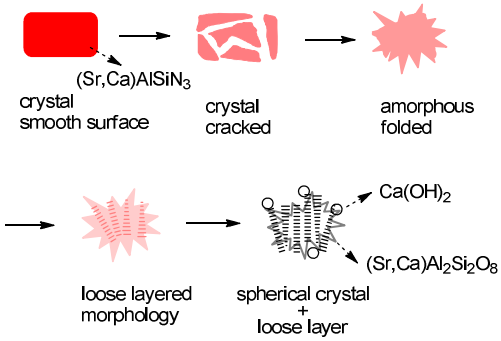

Fig. 10 A schematic mechanism that accounts for the moisture-induce degradation.

In addition, observations of the characteristic Eu^{3+} luminescence and peaks in XPS spectra clearly imply that the oxidation of Eu^{2+} also occurs during the treatment. It also has been reported for $SrSi_2O_2N_2$:Eu and $BaMgAl_{17}O_{19}$:Eu under the thermal attack. [21, 35-37] The oxidation significantly reduces the concentration of divalent europium, and the resultant trivalent europium may act as traps or killers, both of which quench the luminescence.

Conclusions

Moisture-induced degradation of a technically important red phosphor $(Sr_{0.4}Ca_{0.592})AlSiN_3:Eu_{0.008}$ was investigated by treating the phosphor powder under a severe condition of high-pressure water steam. The luminescence degradation occurred at 150°C and went fast thereafter, resulting in the bleaching of the phosphor body color. The activation energy for the degradation was calculated as 66.32 kJ. By means of a variety of analytic techniques, it is understood that the moisture-induced degradation was caused by the oxidation of both the phosphor host and activator (Eu^{2+}) via an oxidant-gas penetration mechanism.

Although it is not a standard accelerated aging test, investigations on phosphors under the high-pressure water steam attack (high humidity, high temperature), quite similar to the Pressure Cooker Test (PCT), will provide some useful information on design, selection and modification of phosphors. It may also save a lot of time to evaluate the aging behavior of a phosphor for solid state lighting.

Acknowledgements

The financial supports of the JSPS KAKENHI (no. 23560811) and the National Natural Science Foundation of China (no. 51272259) are acknowledged.

Notes and references

[a] Sialon Group, Sialon Unit, National Institute for Materials Science, Namiki 1-1, Tsukuba, Ibaraki 305-0044, Japan.
[b] School of Chemical Engineering, Nanjing University of Science and Technology, 200 Xiao Ling Wei, Nanjing, Jiangsu 210094, China.
[c] College of Materials, Xiamen University, Xiamen, Fujian 361005, China.
[d] Nano Device Characterization Group, National Institute for Materials Science, Namiki 1-1, Tsukuba, Japan.
[e] Graduate School of Pure and Applied Science, University of Tsukuba, Tenodai 1-1-1,Tsukuba, Ibaraki 305-8571, Japan.
Electronic Supplementary Information (ESI) available: See DOI: 10.1039/b000000x/

1 N. Grassie and Scott, G. *Polymer degradation and stabilization*, New York, NY: Cambridge University Press; **1985**.
2 B. Singh and N. Sharma, *Poly. Degrad. Stab.*, 2008, **93**, 561-584.
3 R.-J. Xie, Y. Q. Li, N. Hirosaki and H. Yamamoto, *Nitride Phosphors and Solid-State Lighting*, CRC Press, Boca Raton, 2010.
4 R.-J. Xie and H. T. Hintzen, *J. Am. Ceram. Soc.*, 2013, **96**, 665-687.
5 M. Zeuner, S. Pagano and W. Schnick, *Angew. Chem. Int. Ed.*, 2011, **50**, 7754-7775.
6 J. Botterman, K. Van den Eeckhout, A. J. J. Bos, P. Dorenbos and P. F. *Smet, Opt. Mater. Express*, 2012, **2**, 341-349.
7 C. C. Yang, C. M. Lin, Y. J. Chen, Y. T. Wu, S. R. Chuang, R. S. Liu and S. F. Hu, *Appl. Phys. Lett.*, 2007, **90**, 123503:1-123503:3.
8 H. A.Hoppe, H. Lutz, P. Morys, W. Schnick and A. Seilmeier, *J. Phys. Chem. Solids*, 2000, **61**, 2001-2006.
9 R.-J. Xie, N. Hirosaki, T. Suehiro, F. F. Xu and M. Mitomo, *Chem. Mater.*, 2006, **18**, 5578-5583.
10 Y. Q. Li, J. E. J. an Steen, J. W. H. van Krevel, G. Botty, A. C. A. Delsing, F. J. DiSalvo, G. de With and H. T. Hintzen, *J. Alloys Compd.*, 2006, **417**, 273-279.
11 R.-J. Xie, N. Hirosaki, M. Mitomo, Y. Yamamoto, T. Suehiro and K. Sakuma, *J. Phys. Chem. B*, 2004, **108**, 12027-12031.
12 R.-J. Xie, N. Hirosaki, M. Mitomo, K. Takahashi and K. Sakuma, *Appl. Phys. Lett.*, 2006, **88**, 101104:1-101104:3.
13 N. Hirosaki, R.-J. Xie, T. Sekiguchi, Y. Yamamoto, T. Suehiro, and M. Mitomo, *Appl. Phys. Lett*. 2005, **86**, 211905:1-211905:3.
14 K. Uheda, N. Hirosaki, Y. Yamamoto, A. Naito, T. Nakajima, H. Yamamoto, *Electrochem. Solid-State Lett.*, 2006, **9**, H22-H25.
15 Y. Q. Li, N. Hirosaki, R.-J. Xie, T. Takeda and M. Mitomo, *Chem. Mater.*, 2008, **20**, 6704-6714.
16 J. W. Li, T. Wanatabe, N. Sakamoto, H. Wada, T. Setoyama, M. Yoshimura, *Chem. Mater.* 2008, **20**, 2095-2105.
17 H. Wanatabe, M. Imai and N. Kijima, *J. Am. Ceram. Soc.*, 2009, **92**, 641-648.
18 K. Sakuma, N. Hirosaki, N. Kimura, M. Ohashi, R.-J. Xie, Y. Yamamoto, T. Seuhiro, K. Asano and D. Tanaka, *IEICE Trans.Electron.* 2005, **E88-C**, 2057-2064.
19 X. Piao, K. Machida, T. Horikawa, H. Hanzawa, Y. Shimomura and N. Kijima, *Chem. Mater.* 2007, **19**, 4592-4599.
20 C. W. Yeh, W. T. Chen, R. S. Liu, S. F. Hu, H.S. Sheu, J. M. Chen and H. T. Hintzen, *J. Am. Chem. Soc.* 2013, **134**, 14108-14117.
21 C. Y. Wang, R.-J. Xie, F. Z. Li and X. Xu, *J. Mater. Chem. C*, 2014, **2**, 2735-2742.
22 Y. D. Li, L. Y. Xiao, Y. L. Liu, P. F. Ai and X. B. Chen, *Sci. Technol. Adv. Mater.*, 2010, **11**, 045003:1-045003:5.
23 R. I. Hegde, P. J. Tobin, K. G. Reid, B. Maiti and S. A. Ajuria, *Appl. Phys. Lett.*, 1995, **66**, 2882-2884.
24 P. D. Kirsch and J. D. Ekerdt, *J. Vac. Sci. Technol., A*, 2001, **19**, 2222-2231.
25 F. Moulder, W. F. Stickle, P. E. Sobol, K. D. Bomben, *Handbook of X-ray photoelectron Spectroscopy*, ULVAC-PHI, inc.370 Enzo, Chigasaki 253-8522 Japan, 1995.
26 C. D. Wagener, W. N. Riggs, L. E. Davils and J. F. Moulder, *Handbook of X-ray photoelectron Spectroscopy*, Perkin- Elmer Corporation, Minnesota, 1979.
27 J. Kloprogge, L.V. Duong, B. J. Wood and R. L. Frost, *J. Colloid Interface Sci.*, 2006, **296**, 572-576.
28 S. Kishida, H. Tokutaka, F. Toda, H. Fujimoto, W. Futo, K. Nishimori and N. Ishihara, *Jpn. J. Appl. Phys*. 1990, **29**, 438-440.
29 F. Mercier, C. Alliot, L. Bion, N. Thromat and P. Toulhoat, *J. Electron. Spectrosc. Relat. Phenom.* 2006, **150**, 21-26.
30 E. J. Cho and S. J. Oh, *Phys. Rev. B*, 1999, **59**, R15613- R15616.
31 J. F. Qi, T. Matsumoto, M. Tanaka and Y. Masumoto, *J. Phys. D: Appl. Phys*. 2000, **33**, 2074-2078.
32 Y. Ikeda and K. Nii., *Boshoku Gijutsu*, 1982, **31**, 156-163.

33 Y. Ikeda and K. Nii., *Oxid. Met*. 1978, **12**, 487-502.
34 K. Honda, T. Maruyama, T. Atake and Y. Saito, *Oxid. Met*. 1992, **38**, 347-363.
35 G. Bizarri and B. Moine, *J. Lumin*. 2005, **113**, 199-213.
36 K. B. Kim, K. W. Koo, T. Y. Cho and H. G. Chun, *Mater. Chem. Phys*. 2003, **80**, 682-689.
37 T. Justel, H. Lade, W. Mary, A. Meijerink and D. U. Wiechert, *J. Lumin*. 2003, **101**, 195-210.

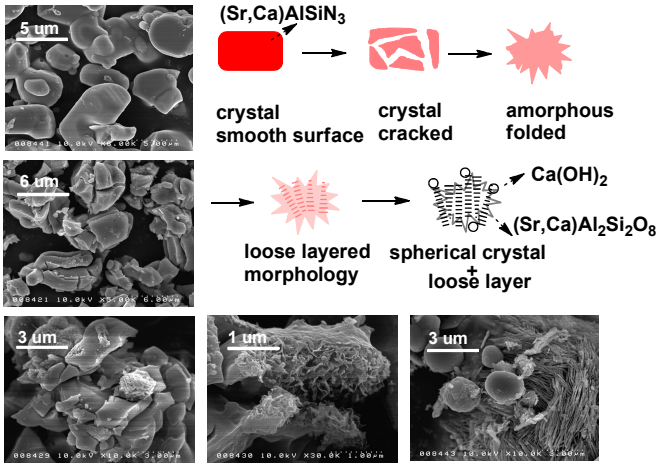

Degradation of (Sr, Ca)$AlSiN_3$:Eu^{2+} induced by the water steam attack results in remarkable changes in luminescence, microstructure and phase purity.